

PIV STUDY OF NEAR WALL ORGANIZED MOTIONS

**Diederichs V., Lapolla M., Loreface L., Malvano R., Palio B., Spazzini P.G., Onorato M.
Haigermoser C., Vesely L.
Politecnico di Torino, Corso Duca Degli Abruzzi 24, Torino, Italy**

Keywords: *turbulent boundary layer, coherent structure, PIV*

ABSTRACT

The strong development of Particle Image Velocimetry in the last few years has opened a new field for the experimental study of turbulent flows. The main importance of PIV with respect to classical point measurement techniques is the ability of producing instantaneous maps of the velocity field, giving information about organized motions and their relation to the skin friction growth and turbulence production. At the Politecnico di Torino Aerodynamic Laboratory a large number of students and researchers is involved in PIV studies on the dynamics of the organized motions in near wall turbulent flows and on their control [6, 7, 9, 10, 15]. In the present paper swirling motions in streamwise-wall-normal planes are described, with reference in particular to the rarely commented positive swirling motions.

1 INTRODUCTION

PIV, as well as Direct Numerical Simulation, has contributed in recent years to the understanding of the dynamics of near wall motions, nevertheless fundamental aspects of the physical behaviour of near wall turbulence remain unsolved. First of all the mechanisms of regeneration of the vortical structures, either by instability of the velocity streaks or by strong shears generated by previous vortical structures or by other mechanisms not yet explored. Besides this fundamental aspects, many other unsolved problems still need experimental (and numerical) work; examples among others are the mechanisms of vortex packets merging and the related coalescence of the low speed streaks, the scale growth with distance from the wall and its possible self-similar behaviour, the influence of the physical state of the wall and of the external flow on the eddy structure.

The study of organized swirling motions in planes (x,y) normal to the wall and streamwise oriented, originated by cutting three-dimensional vortical structures with the PIV measurement plane, has been the subject of many investigations, among others, see references [1, 2, 8, 11, 12, 13, 14, 15, 16].

In this paper results will be shown concerning the dynamics of swirling motions in planes (x,y) and in particular concerning the presence of vortical motions having positive spanwise vorticity. The sign of the mean boundary layer spanwise vorticity is here defined as negative.

2 EXPERIMENTAL SET UP AND ANALYSIS METHOD

The experiments were carried out in the water tunnel at the “Dipartimento di Ingegneria Aeronautica e Spaziale” of the Politecnico di Torino. This facility is a closed-loop open-flow channel with a 350 x 500 x 1800 mm³ test section. The external free-stream turbulence was 2%.

Measurements were taken on a flat plate with a length of 2050 mm. At the leading edge the transition was imposed by sand paper.

Measurements were taken with a PIV System, which consisted of a Nd: YAG, Q-switched laser, with 200 mJ of energy per pulse and a pulse duration of 5-6 ns, providing a double-pulsed

beam, a 1280x1024 pixels CCD Camera (PCO Sencam) with a focal length of 105mm and a DANTEC system hub for synchronizing the acquisition. The laser beams were expanded by a cylindrical lens and focused by a spherical lens, forming a light sheet with a thickness of about 0.5 mm. The water was seeded with spherical solid particles, 2 μm nominal diameter, which were small enough to follow the flow faithfully. The density of the particles was high enough to allow performing correlation algorithms. The local particle image displacements were determined using an adaptive cross-correlation algorithm. The final interrogation window size was 32x32 pixels, corresponding to 14 x 14 viscous units.

Swirling motions were identified by the method proposed by Zou et al. [18], searching for positive values of the swirling strength λ_{ci} of the vortex.

The boundary layer flow at the measurement section was characterized by $Re_\theta=1060$, $H=1.47$, $U_e/u_\tau=21.6$, with $U_e=0.383\text{m/s}$.

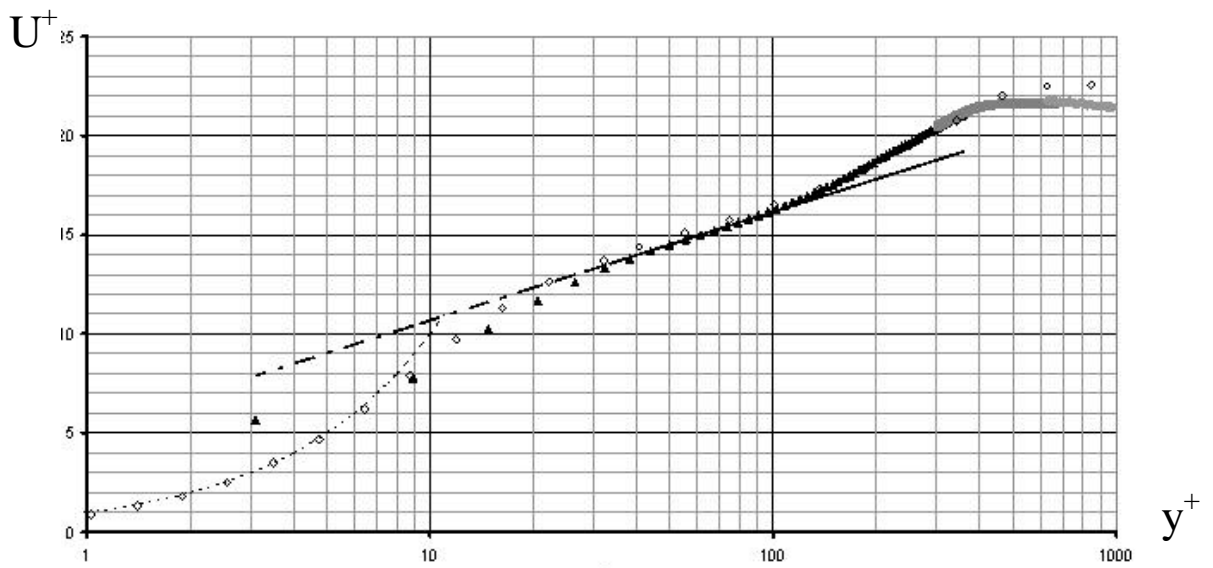


Fig.1 Mean velocity profiles. Full symbols: PIV results. Empty symbols: LDV results.

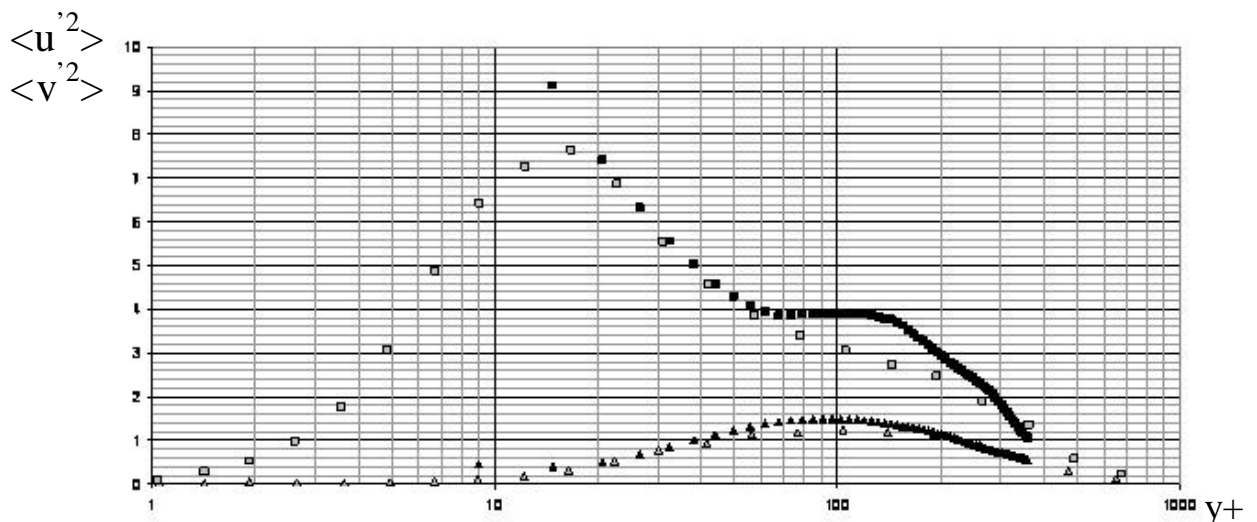


Fig.2 Velocity variance profiles. Full symbols: PIV results. Empty symbols: LDV results.

3 RESULTS

The mean velocity profile in semi-logarithmic axis is shown in Fig.1, plotted in inner-scaling variables. The experimental data compares satisfactory with LDV data obtained by DeGraaf & Eaton [5] at $Re_\tau=1430$. The variance of the longitudinal and wall normal velocities, $\langle u'^2 \rangle$ and $\langle v'^2 \rangle$, are shown in Fig.2. The figure also shows data obtained by DeGraaf & Eaton. The fit between the two sets of data for the longitudinal-velocity component is good over the range $y^+ = 20$ to $y^+ = 55$. The PIV data shows a plateau of constant $\langle u'^2 \rangle^+$, equal to 3.9, between $y^+ = 55$ and $y^+ = 135$, from which the value of $\langle u'^2 \rangle^+$ decreases rapidly to 1.1 at $y^+ = 350$. This behaviour is not mimicked by the LDV data and is typical of higher Reynolds number flows and (or) of higher levels of the free stream turbulence [3]. For the present experiments the free stream turbulence was 2%, much higher than in the DeGraaf & Eaton experiments. The wall-normal velocity fluctuations are also greater for the present data than that of DeGraaf & Eaton in the range $y^+ = 30$ to $y^+ = 180$.

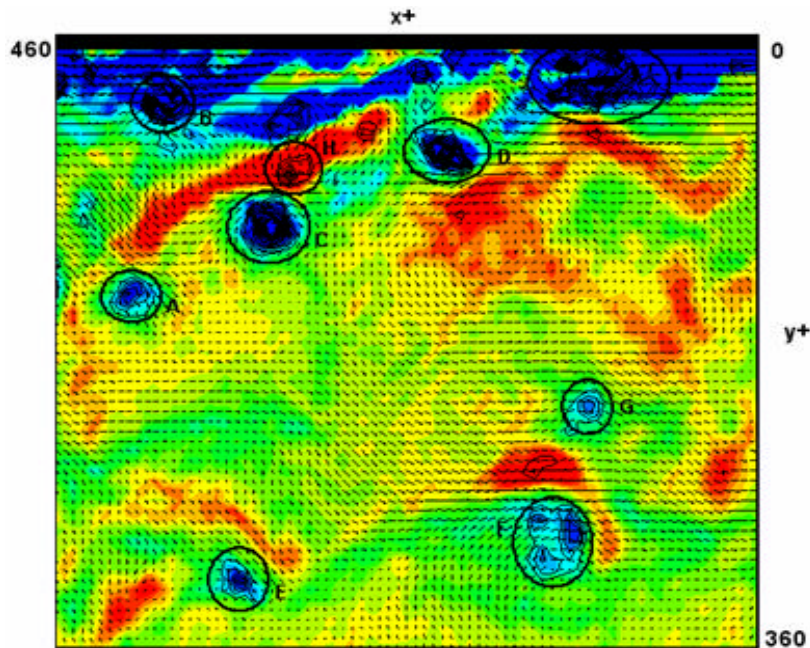
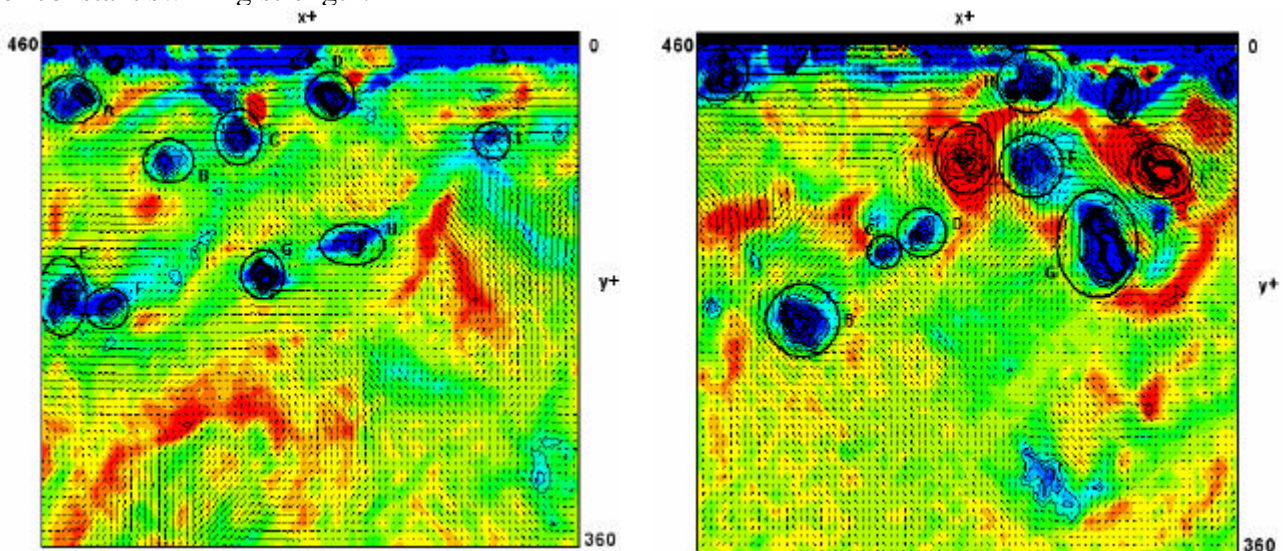


Fig.3 Instant PIV image. Vectors: fluctuating velocity field. Colour map: vorticity. Isolines: lines of constant swirling strength.



Figs.4 and 5 Instant PIV images.

Fig.3 shows a typical PIV image. The mean flow comes from right to left and the wall is at the top of the image. The image shows inclined shear layers, or vorticity sheets, as well as a train of negative (blue) vortices, A, C, D and I, extending from the near-wall region to beyond the logarithmic region. This arrangement of the vortices conforms to the Packet model proposed by Adrian *et al.*[2]. The image also shows a further possible packet of vortices, E, F and G in the outer layer. The velocity vectors indicate quadrant events, with a large proportion of Q2 and Q4 events. The image also contains a positive (red) swirling motion, H, situated between negative vortex C and the negative shear layer. This vortex cannot be extracting energy from the mean shear directly, and its presence has not previously been documented, except recently by Christensen & Wu [4]. Analysing the present results significant numbers of positive vortices like the one in Fig.3 were observed. The convection velocities of each vortex was determined by performing a Galilean decomposition and altering the convection velocity, \mathbf{U}_c , such that the velocity vectors showed a clear circular pattern with a stagnation point at the centre. The convection velocities of A, C, D and I respectively are, 0.29 m/s, 0.29 m/s, 0.3 m/s and 0.19 m/s. This confirms that A, C and D are travelling coherently as a packet and that I may be part of this packet or may be a separate vortex that has been over-run by this packet. Similar vortical organizations are shown in figures 4 and 5. A near wall packet extending through the logarithmic region and an outer layer packet are reported in Fig.4. A large packet, comprising of 5 negative vortices, extending from the near-wall region to the outer layer is evident in Fig.5, where also two positive swirling motions are detected.

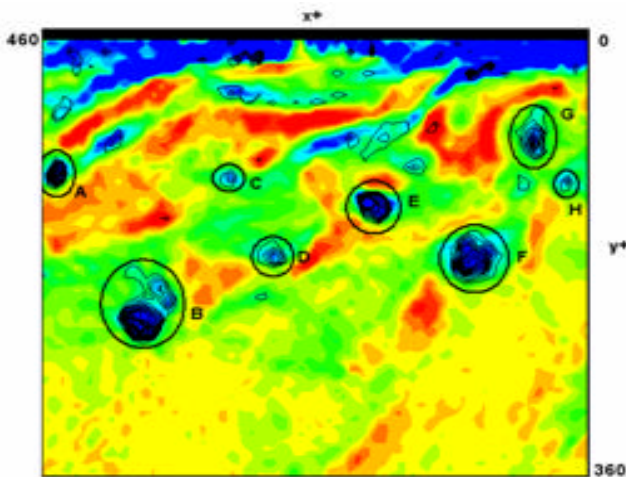


Fig. 6a Instant PIV image.

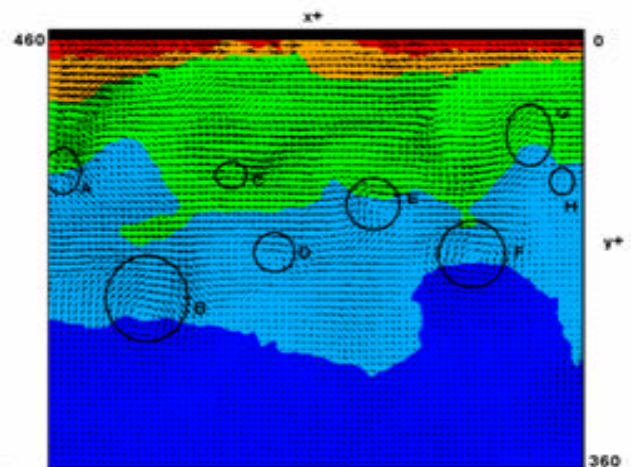


Fig. 6b Uniform momentum zones.

Inclined shear layers have been noted in many previous studies of the turbulent boundary layer. Fig.6a shows shear layers of alternating vorticity, inclined to the wall. Adrian *et al.* relates these shear layers to zones of uniform momentum, as displayed in Fig.6b, where the uniform momentum zones are evidenced by colour map of $(U-0.8U_c)/u_t$, a quantity used by Adrian *et al.* to visualise the zones. The majority of the swirling motions present in Fig.6b are, as expected, located on the border between uniform momentum zones, in particular vortices A, B, E, F, G and H. The shear layers of negative vorticity appear on Fig.6b as ‘dark’ regions, i.e. regions of large velocity vectors; this is in accordance with the findings of Smith & Metzler [17]. Many similar images may be found in the present data set. These shear layers are indicated by Meinhart & Adrian. [14] as possible initial mechanism of the generation of packets of vortical structures by a mechanism of vorticity roll-up.

Significant numbers of positive (red) vortices were observed in the collected images of the present results. According to Christensen & Wu the presence of significant numbers of positive vortices is a new finding in canonical wall turbulence. Positive vortices are not present in either the

Adrian et al. hairpin vortex model or the model proposed by Jeong *et al.* [11] involving train of quasi-streamwise vortices, nor can they be extracting energy directly from the mean shear. Christensen & Wu propose that the positive vortices are formed by intense regions of local shear, such as those e.g. that exist between two negative vortices. This mechanism is evident in many images of the present data set, such as that shown in Fig.7, where multiple negative vortices A, B, C, E and I, K produce strong opposing quadrant events which induce positive mean shears resulting in secondary positive vortices G, E and J.

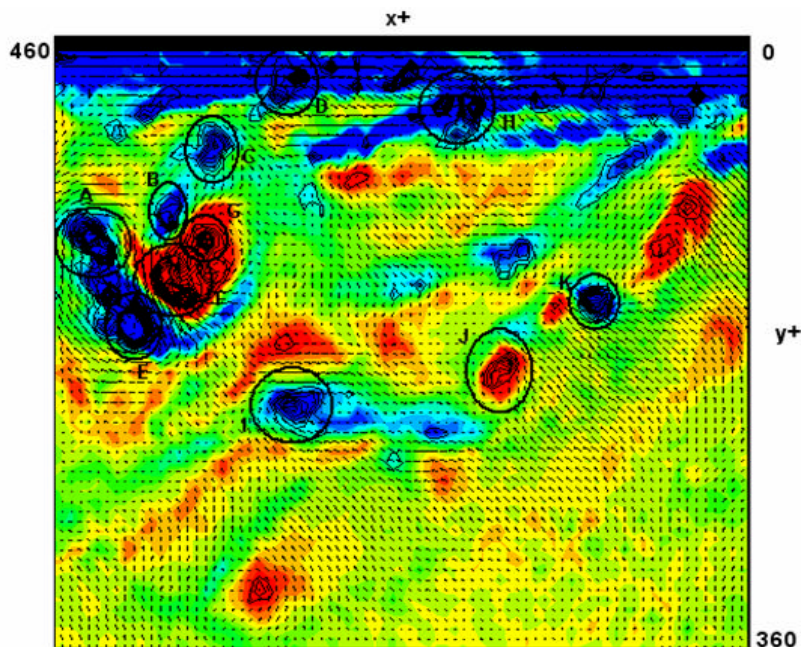


Fig.7 Instant PIV image.

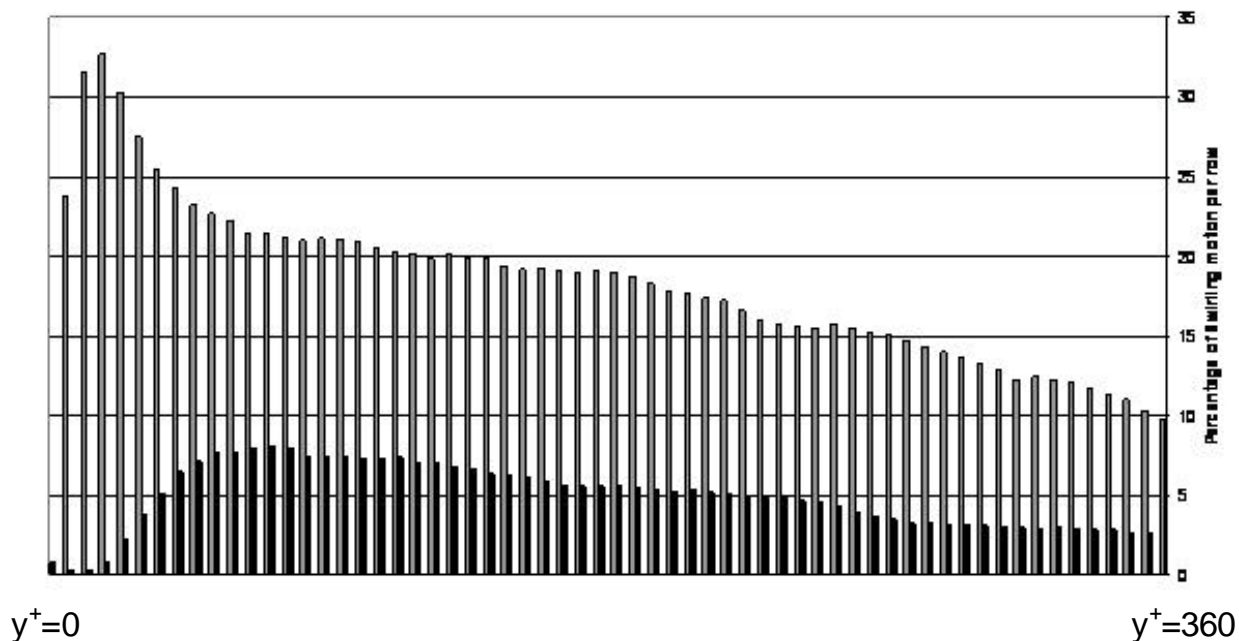


Fig.8 Percentage of measurement points involved in swirling motions in function of the distance from the wall. Empty bars: negative vorticity. Full bars: positive vorticity.

Fig.8 is a histogram showing the distribution of points involved in negative and positive swirling motions, whose swirling strength exceeds a given low threshold, as a percentage of the total measurement points, at different distance from the wall. The wall is at the left of the histogram and the right most data bar is at a distance of $y^+ = 360$. The histogram obeys the same trends found by Christensen & Wu, whereby the negative vortices are most abundant close to the wall, attaining a peak at approximately 26 wall units, in the buffer layer, with the percentage reducing as distance from the wall increases. Although the percentage of vortices decreases in the external portion of the boundary layer, over ten percent of the outer layer is involved in a negative swirling motion. The distribution of positive vortices presents a peak at $y^+ = 77$, which is further from the wall than the peak of negative vortices. These findings are in line with those of Christensen & WU who hypothesised that the negative vortices form at the wall, whilst the positive vortices form away from the wall, and in both cases ascend into the external portion of the boundary layer.

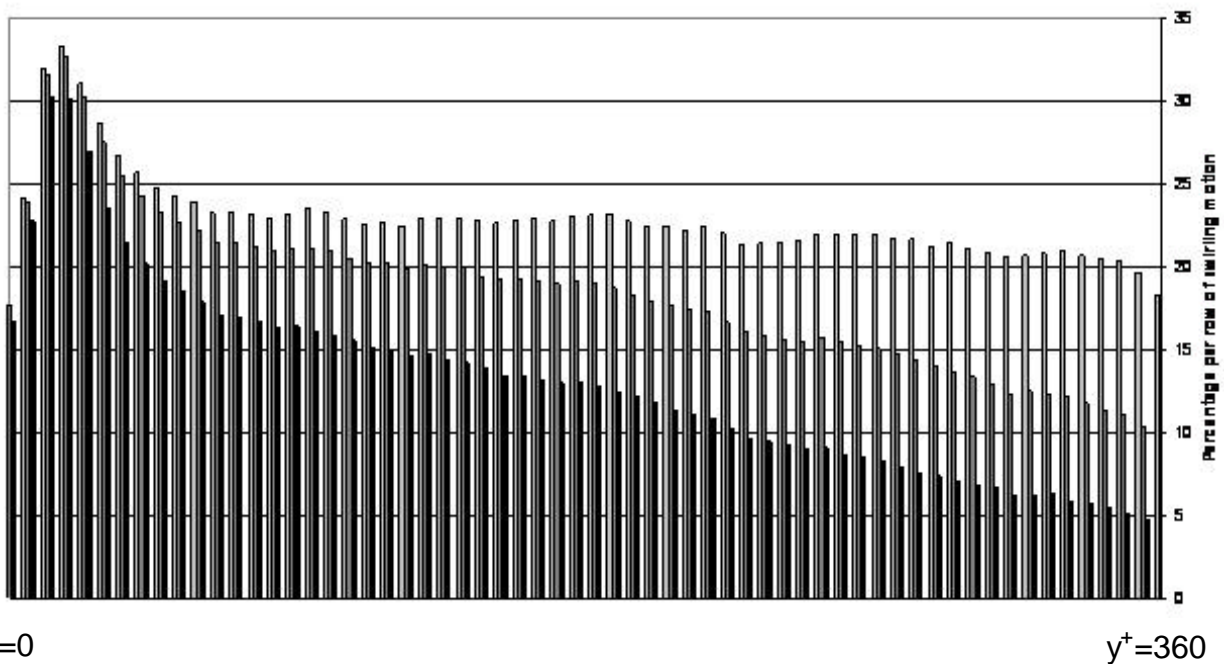


Fig.9 Percentage of measurement points involved in negative swirling motions in function of the distance from the wall, for different swirling strength. The threshold increases from empty bars to full gray bars to full black bars.

By altering the threshold level it was possible to remark on the strength of the vortices, as a strong vortex will be present even if the threshold level is increased, whilst a weak vortex will be excluded by a larger threshold. Fig.9 and Fig.10 show the results of such variation on the distribution of respectively negative and positive vortices. Negative vortices (Fig.9) near the wall are strong, as the percentages recorded near the wall appear relatively unaffected by the change in threshold, however as the distance from the wall increases more and more vortices are excluded by the increased threshold level, suggesting that not only does the number of vortices decrease as the distance from the wall increases, but the vortices are becoming weaker. Fig.10 shows that the positive vortices are formed away from the wall, as proposed by Christensen & Wu, and that they ascend into the external portion of the boundary layer, weakening as they ascend. Moreover it is also evident that the positive vortices are weaker than the negative vortices, as the ratio between positive and negative vortices decreases as the threshold is increased, implying that more positive vortices are being excluded than negative vortices.

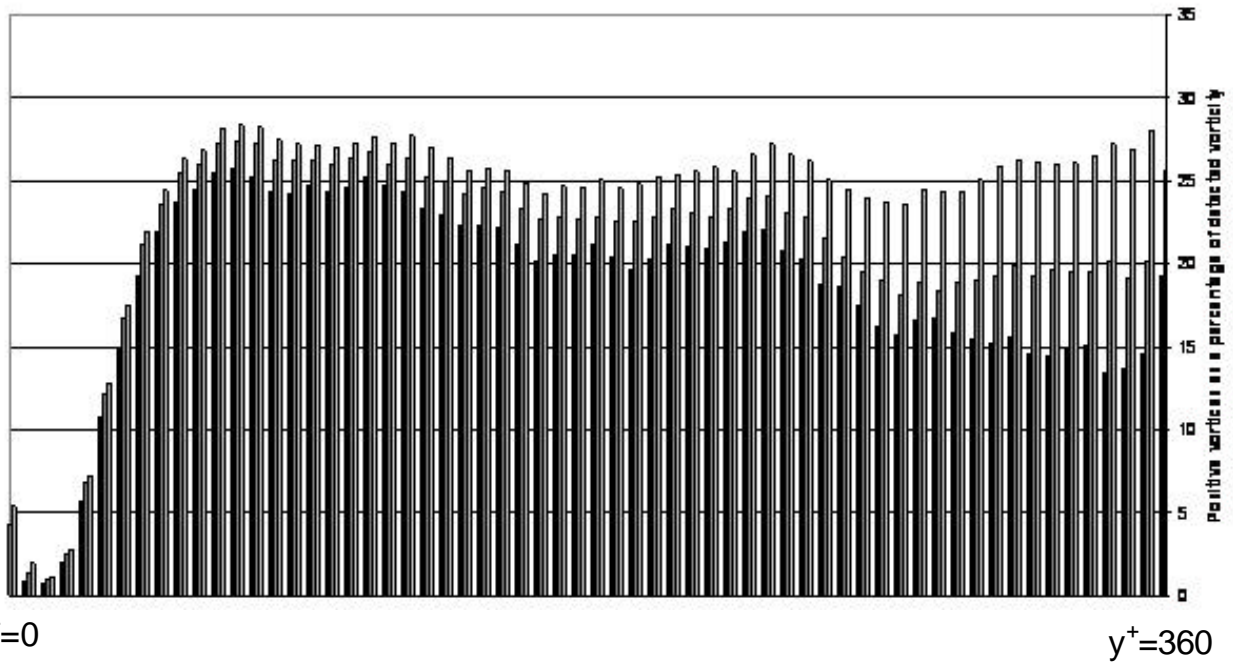


Fig.9 Percentage of measurement points involved in positive swirling motions in function of the distance from the wall, for different swirling strength. The threshold increases from empty bars to full gray bars to full black bars.

CONCLUDING REMARKS

The described boundary layer structures confirm previous studies: inclined shear layers, quadrant events, vortical structures and low momentum zones were noted in abundance in the data set. The arrangement of these structures was, as expected, with vortical structures occurring on the boundaries of low momentum zones, and quadrant events were generated adjacent to vortical structures. In addition strong quadrant-2 or quadrant-4 events were observed near strong vortices, or in regions where numerous vortices were working together.

A relatively new finding was the appearance of significant numbers of positive vortices. These vortices cannot be extracting energy directly from the mean shear, and nor can they be the result of cutting through a cane-like or hairpin vortex model (Adrian *et al.*) or through the alternating quasi-streamwise vortical structures model (Jeong *et al.*). The generation of positive vortices was clearly observed during these tests according to an induction model, whereby two negative vortices induce a region of positive shear between them that leads to the re-circulation of a positive vortex. Future studies should focus on the role of these vortices in the boundary layer. Are they involved in turbulence production? Are they involved in the generation of negative vortices? What is the three-dimensional structure of these vortices? Is the structure random or does a dominant structure form?

Distributions of points involved in swirling motions, both negative and positive, were generated so that conclusions could be drawn on their location with respect to the wall and strength. A peak in both number of points detected and strength was noted at $y^+ = 26$, for the negative vortices and at $y^+ = 77$ for the positive vortices. It is possible to conclude that the negative vortices are formed at the wall, whilst the positive vortices are generated further from the wall. Subsequent to their formation the vortices ascend into the external part of the boundary layer, weakening as they ascend. 25% of the vorticity within vortices was noted to be positive, which quantitatively confirms the induction model and the findings of Christensen & Wu.

REFERENCES

1. Adrian R.J., Christensen K.T., Liu Z.C. *Analysis and interpretation of instantaneous turbulent velocity fields* Experiments in Fluids 29, pp. 275-290, 2000.
2. Adrian R. J., Meinhart C. D., Tomkins C.D. *Vortex organisation in the outer region of the turbulent boundary layer*, J. Fluid Mechanics 422, pp.1-54, 2000.
3. Castro I.P. *Effects of free stream turbulence on low Reynolds number boundary layers*. Journal of Fluids Engineering 106, pp. 298-306, 1984.
4. Christensen K. T., Wu Y. *A population study of small-scale spanwise vortices in turbulent channel flow*, 11th International Symposium on Flow Visualization, 2004.
5. DeGraaf D.B., Eaton J.K. *Reynolds-number scaling of the flat-plate turbulent boundary layer*. J. Fluid Mechanics, 422 pp. 319-346, 2000.
6. Di Cicca G.M., Iuso G., Spazzini P.G., Onorato M. *PIV study of the influence of large-scale streamwise vortices on a turbulent boundary layer*, Experiments in Fluids 33, pp.663-669, 2002.
7. Di Cicca G.M., Iuso G., Spazzini P.G., Onorato M., *Particle image velocimetry investigation of a turbulent boundary layer manipulated by spanwise wall oscillations*, J. Fluid Mechanics 467, pp: 41, 2002.
8. Ganapathisubramani B. Longmire E.K., Marusic I. *Characteristics of vortex packets in turbulent boundary layers*, J. Fluid Mech. 478, pp. 35-46, 2003.
9. Gottero M. and Onorato M. *Low-speed streak and internal shear layer motions in a turbulent boundary layer*, Eur. J. Mech. B-Fluids 19, 2000.
10. Iuso G., Di Cicca G. M., Onorato M., Spazzini P. G., Malvano R. *Velocity streak structure modifications induced by flow manipulation*. Physics of Fluids, vol. 15, number 9, pp 2602-2612, 2003.
11. Jeong J., Hussain F., Schoppa W., Kim J. *Coherent structures near the wall in a turbulent channel flow*. J. Fluid Mechanics, 332 pp. 185-214, 1997.
12. Jiménez J., Pinelli A. *The autonomous cycle of near-wall turbulence*. J. Fluid Mechanics, 389 pp. 335-359, 1999.
13. Liu Z., Adrian R.J., Hanratty T.J. *Large-scale modes of turbulent channel flow: transport and structure*, J. Fluid Mech. 448, pp. 53-80, 2001.
14. Meinhart C.D., Adrian R.J. *On the existence of uniform momentum zones in a turbulent boundary layer*, Phys. Fluids 7, pp. 694-696, 1995.
15. Onorato M., Di Cicca G. M., Iuso G., Spazzini P. G., Malvano R., *Turbulent boundary layers and their control: quantitative flow visualization results*. World Scient.Publ., pp. 247-282, 2006.
16. Schoppa W., Hussain F., *Coherent structure generation in near-wall turbulence*. J. Fluid Mechanics, 453, pp. 57-108, 2002.
17. Smith C.R., Metzler S.P., *The characteristics of low speed streaks in the near-wall region of a turbulent boundary layer*. J. Fluid Mechanics, 129, pp. 27-54, 1983.
18. Zhou J., Adrian R.J., Balachandar S., Kendall M.T., *Mechanisms for generating coherent packets of hairpin vortices in channel flow*. J. Fluid Mechanics, 387, pp. 353-396, 1999.